Experimental investigation of corrosion behaviour in Al alloy reinforced with SiC functionally graded composite

S. Prathap Singh*, *K* Gnanasekaran, *Roshan* Santhosh, and *U* Srikanth

Department of Mechanical Engineering, St. Joseph's Institute of Technology, Chennai, Tamil Nadu, India

Abstract. The corrosion behavior of Al6061 alloy reinforced with 10 wt.% Silicon Carbide (SiC) particles in a Functionally Graded Composite (FGC) that was produced using vertical centrifugal casting and stir casting techniques is the primary focus of this investigation. The microstructural analysis demonstrated a distinct gradient in the distribution of ceramic particles, which led to low, intermediate, and high particle concentration zones throughout the cross section. The highest hardness was confirmed in the high particulate concentration zone by Vickers microhardness testing, which was attributed to enhanced ceramic dispersion. The corrosion performance of a Taguchi L9 orthogonal array was assessed in acidic media, including hydrochloric acid (HCl), sulphuric acid (H_2SO_4), and nitric acid (HNO_3), at varying plunging durations and distances from the boundary edge. The results indicate that the Corrosion Rate (CR) was significantly influenced by the acid type and plunging durations. The CR was at its highest in HCl and decreased as the immersion duration increased as a result of the formation of passive layers. The CR increased as the distance from the boundary margin increased, as a result of the weaker development of passive layers in the inner areas and the lower ceramic content.

1 Introduction

The seamless transition of material composition and attributes within a component has made FGCs more popular in recent years. This, in turn, mitigates challenges associated with interfacial stress concentrations and enhances overall performance in applications such as corrosion protection, abrasion resistance, and mechanical strength [1,2]. The potential to enhance mechanical properties has been demonstrated by the gradient structure of Al6061-based FGCs that are reinforced with ceramic particles, including SiC, Alumina (Al_2O_3), and Boron Carbide (B_4C) [3, 4]. FGCs were produced by Karabulut et al. through the use of centrifugal and agitation casting. They discovered that the ballistic and mechanical performance of Al6061-based FGCs was enhanced by the gradient distribution of reinforcements such as SiC.

* Corresponding author: prathap.singh50@gmail.com

Corrosion behavior in extremely hostile environments is a major concern for Al6061 composites. The effects of SiC composition and testing conditions on CRs are substantial, according to studies of conventional homogeneous Al6061/SiC composites. Using the Taguchi design-of-experiments method, Sarapure et al. demonstrated that Al6061's corrosion resistance under NaCl conditions was enhanced by increasing the SiC content to up to 4 wt.%. Immersion time, solution normality, and SiC weight percentage were the most notable features [6]. Similarly, Al6061 and Al5052 reinforced with 5-10 wt% were investigated by Uday et al. Solution concentration, exposure time, and SiC content were found to have a significant impact on the corrosion behavior of Sodium Chloride (NaCl). In contrast to FGCs, which have an optimally distributed reinforcement, homogeneous composites might experience localized corrosion. The effect of gradient structuring on the characteristics of different areas was demonstrated by the enhanced hardness and wear resistance of continuous graded Al alloy/SiC composites made by centrifugal casting from the inside outwards [7]. Graded reinforcement is useful for changing mechanical and tribological behaviors, as demonstrated by the improved wear performance of Al6061-based FGCs with progressively added Al_2O_3 layers (ranging from 0 to 50 wt.%), according to research by Rupesh et al. [8].

Notwithstanding these advancements, there is still a dearth of literature concerning the corrosion behavior of functionally graded Al6061/SiC composites. Performance of homogeneous or mechanical/attrition systems has been the primary focus of most prior research. Centrifugal forces promote a preferential deposition of ceramic particles, such SiC, in the outer regions of FGCs created by centrifugal casting, leading to gradation. Because it changes the local microstructure, ceramic composition, particle size, passive film properties, and micro-galvanic interactions. But there is a lack of comprehensive studies that measure these regional differences in corrosion rates.

This study addresses this knowledge gap by analyzing the corrosion behavior of Al6061/SiC FGCs, specifically focusing on the correlation between distance from boundary and CR. Employing centrifugal casting methods to establish gradation, the work involves microstructural characterization, hardness mapping, and systematic corrosion testing at multiple distances from the boundary.

2 Materials and methods

2.1 Materials and fabrication

Al6061 is mostly composed of the following alloying elements: Mg, Si, Cu, Cr, Zn, Ti, Mn, and other elements. Initially, Al6061 alloy was heated in a resistance furnace that used electric current (Figure 1(a)). The SiC particles were carefully added to the 750°C superheated melt by hand. In order to finish the reaction, the molten metal was held for 25 minutes and agitated occasionally using a graphite impeller.

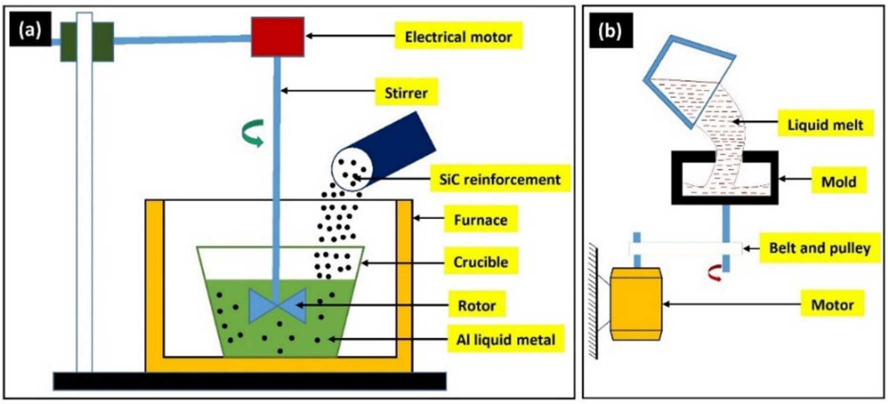

Fig. 1. (a) Sketch of stir casting methodology, and (b) Sketch of vertical centrifugal casting methodology.

Subsequently, a vertical centrifugal mold was used to cast the FGC. A centrifugal mold that spins at 1100 rpm is filled with molten metal during the composite's primary processing step, the molten metal stir casting process (Figure 1(b)). A hollow cylinder made of Al6061-10 wt.% FGC was cast; it has measurements of 50 mm in span, 150 mm in outer diameter, and 105 mm in thickness.

2.2 Mechanical and microstructural characterization

An Olympus upright microscope was utilized to study the morphology and gradient dissemination of hard ceramic strengthening reinforcements on Al6061-10 wt.% FGC at various regions. Wire-cut electric discharge machining was used to cut composite sections from different areas. Abrasive sheets of grid sizes of different sizes ranging from 220, 320, 600, 1000, and 2000 and alumina cloth polished the cut samples. Final polishing was done with 0.5 µm diamond paste. Keller's solution (2.5% HNO_3, 1.5% HCL, 1% HF, and remainder distilled water) was used to etch diamond-polished specimens to study surface morphology. The Vickers microhardness experimentation was performed according to ASTM-E384 from exterior to interior periphery (1 to 45 mm) with 100 gf load for 15 seconds. The Vickers microhardness of the region was averaged from five measurements.

2.3 Corrosion experimentation

The experiment involving acidic exposure corrosion was conducted to assess the corrosion behavior of Al6061-10 wt.% SiC FGC when exposed to diluted acids prevalent in the chemical and acid handling sectors. The corrosion experimentation was conducted in this setting by submerging FGC specimens in 1 M HCl, H_2SO_4, and HNO_3 for an extended period of immersion.

The FGC samples were scrupulously cleaned with acetone and weighed on a precision weight machine that could measure to an accuracy of 0.001 grams prior to the commencement of the experiment. The samples were calibrated to estimate the weight decrease for the CR evaluation after being removed from the acidic solution within the specified interval. The formula for calculating CR in millimetres per year is delineated by Equation (1).

$$CR = \frac{(K \times w)}{(A \times d \times t)} \tag{1}$$

K is the corrosion variable constant (8.76*104), w is the weight loss in grams, A is the exterior surface significantly affected by corrosion in cm^2, d is the density of the fabricated Al6061-10 wt.% FGC test sample in g/cm^3, and t is the time spent immersed in acidic solutions.

Taguchi's L9 orthogonal array provides support for the experimentation design. The Taguchi approach for implementing Design of Experiments (DOE) is basic and understandable. The strategy effectively reduces the scope of research operations to a small number of experiments. This experiment takes into account three corrosion input variables: acidic solution, dipping time, and distance from the border edge. Response is denoted by CR. In Taguchi's methodology, the selection of the appropriate orthogonal array is determined by three key factors: This document describes the important input and response parts, as well as the momentous relations. There are two levels of evidence for input variables. Expected experimentation results, as well as economical and effectiveness limits. Table 1 depicts the 3 contribution variables, each categorised into 3 dissimilar stages, as accepted in the existing works.

Table 1. Levels of input corrosion variables.

Levels	**Acidic Solution**	**Dipping duration (Hours)**	**Distance from boundary edge (mm)**
1	HCl	48	15
2	H_2SO_4	144	30
3	HNO_3	216	45

The plan matrix for trialling is created utilizing the Taguchi methodology within MINITAB 21 software, as visualized in Table 2.

Table 2. Design matrix and investigated outcomes.

Run No	**Acidic Solution**	**Dipping duration (Hours)**	**Distance from boundary edge (mm)**	**CR (mm/year)**
1	HCl	48	15	28.90
2	HCl	144	30	13.07
3	HCl	216	45	11.58
4	H_2SO_4	48	30	14.62
5	H_2SO_4	144	45	11.03
6	H_2SO_4	216	15	3.28
7	HNO_3	48	45	16.90
8	HNO_3	144	15	3.21
9	HNO_3	216	30	9.01

3 Results and discussions

3.1 Vicker's microhardness examination

Figure 2 displays Vickers microhardness measurements on Al6061-10 wt.% SiC FGC, conducted radially from the external to the internal boundary at 5 mm intervals. It decreased correspondingly toward the inner boundary edge. The radial gradient hardness distribution showed a maximum hardness of 5-20 mm from the outer boundary edge, known as the high particle concentration region. This could be due to the movement of higher density SiC to the high particle concentration region. Centrifugal force and density difference result in the attendance of primary SiC elements on the exterior of the FGC. The chilled region formed 5 mm from the exterior due to the molten mixture solidifying quickly at the mold surface. After 30 mm from the outside boundary, the low particle concentration region is formed by small holes and porosities thrown from all casting regions by centrifugal force. The intermediate hardness zone, located between 21 and 29 mm from the outer boundary, is influenced by centrifugal rotation speed. The high particle concentration region had a peak hardness of 120 HV, 62% higher than the low particle concentration region. This is because the alloys improve wettability and ceramic particle dispersion [9].

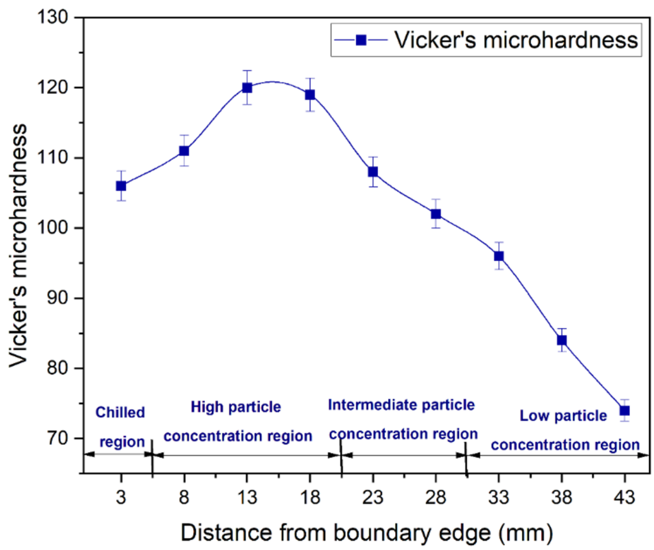

Fig. 2. Increase in Vicker's microhardness from the exterior to the interior region of the Al6061-10 wt.% SiC FGC.

3.2 Microstructural and mechanical characterization

Figure 3 shows the optical microstructure of Al6061-10 wt.% SiC FGC from the outside in. This study authorised the gradient dissemination of SiC hard ceramic strengthening elements and found 4 key zones: chilled, high, intermediate, and low particle concentration region. The gradient arrangement in the FG composite is caused by centrifugal power and melt solidification rate differences in the spinning mold. Figure 3(a) shows the microstructure of the high particle concentration region. High concentration of SiC particles was observed due to centrifugal force. The centrifugal force pushed high-density (3.21 g/cm^3) SiC elements to the outer perimeter, creating a high particle concentration region matched to aluminum A356 alloy (2.7 g/cm^3).

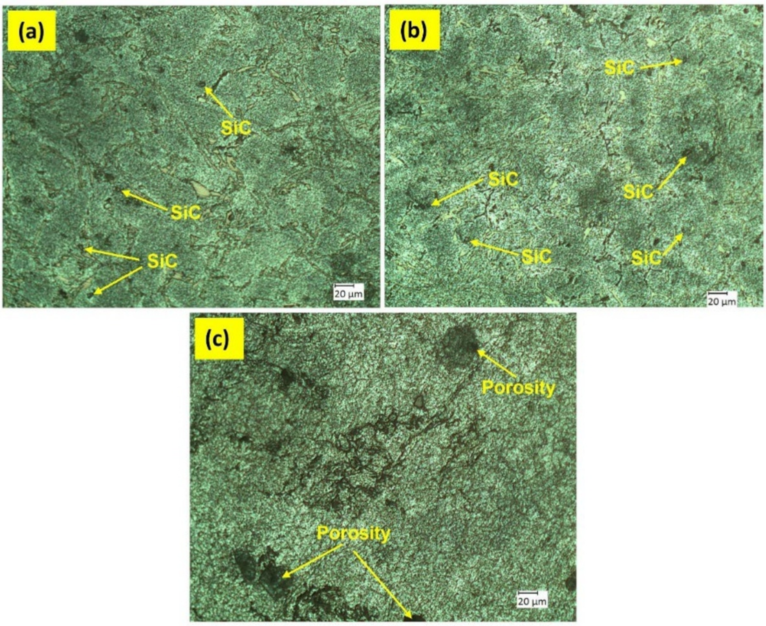

Fig. 3. Optical microstructure to show the particle distribution at (a) High particle concentration region, (b) Intermediate particle concentration region, and (c) Low particle concentration region.

Figure 3(b) displays the intermediate particle concentration region. There were less SiC particles than in the nearby high particle concentration constituency. In Figure 3(c), the microstructure of the low particle concentration region is seen. This section along the inner edge has a depletion of reinforcement particles.

3.3 Statistical analysis of CR

The response table for SNR was acquired by Minitab software from the SNRs of their equivalent CR measurements. Table 3 demonstrations the rank of impact of the corrosion controlling variables such as acidic solution, immersion time, and different zones on the CR. The delta assessment evaluated the impact of the corrosion variable. The delta number was designed by subtracting the maximum and minimum SNR of the corrosion controlling variables. The impact of immersion time on the CR was found maximum continued by the impression of acidic solution and different zones identified from outer periphery of the FGC.

Table 3. Response Table for SNRs of the CR.

Level	Acidic Solution	Immersion time	Zone from outer periphery
1	-18.16	-25.69	-16.56
2	-24.27	-17.77	-21.57
3	-17.93	-16.90	-22.23
Delta	6.34	8.79	5.67
Rank	2	1	3

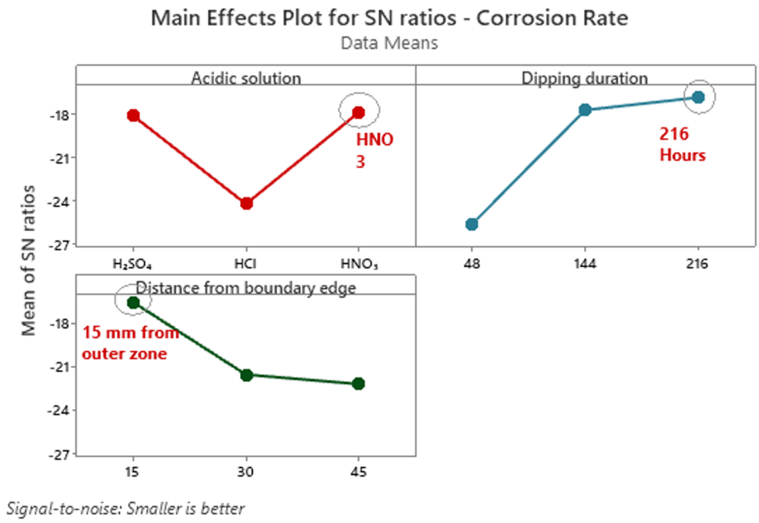

Fig. 4. SNR response graph for the CR to study the influence of corrosion variables.

The graphs designed for CR and the SNRs are publicized in Figure 4 where the maximum SNRs for each corrosion controlling variables provides the optimum set of corrosion variables. The optimum set of corrosion variables to achieve minimum CR was detected at an acidic solution of HNO_3, dipping duration of 216 hours and the zone from the boundary edge of 1 mm.

Table 4. ANOVA outcome for the CR.

Source	DF	Adj SS	Adj MS	F-Value	P-Value	Contribution percentage (%)
Acidic solution	2	133.651	66.825	1.87	0.348	27.87
Dipping duration	2	271.555	135.777	3.81	0.208	56.63
Different zone from boundary edge	2	2.942	1.471	0.04	0.960	0.61
Error	2	71.364	35.682			14.89
Total	8	479.512				

Analysis of Variance (ANOVA) was utilized to conclude the importance stage of the corrosion variables and is revealed in Table 4. Confidence percentage of 95 was fixed for the exploration. The level of importance on CR was supreme for dipping duration (56.63%) continued by acidic solution (27.87%) and different zone from boundary edge (0.61%). The percentage contribution of corrosion variables on the SR is high for dipping duration. The P-values from the ANOVA findings (Table 4) exceed 0.05, suggesting that the components' effects are statistically inconsequential at the 95% confidence level, but the observed trends are nevertheless useful for assessing each corrosion variable's contribution percentage.

3.4 Consequence of corrosion variables on the CR

Figure 5 illustrates the influence of different corrosion control variables on the CR. From the Figure 5, the FGC samples immersed in HCl acidic solution revealed the maximum CR of 17.85 mm/year, which is higher than the CR observed in the samples immersed in H_2SO_4 and

HNO_3. The FGC sample dipped HCl acidic mixture experienced the most pronounced effect, possibly due to its strong reactivity and ability to aggressively attack the surface. Conversely, H_2SO_4 and HNO_3 may generate passive layers or interactions that are less aggressive. Corrosion is substantially enhanced when FGCs are submerged in HCl acidic solutions that contain chloride ions. Chloride ions are generated in the HCl solution through the process of water ionization. Chloride ions initially impair the FGC's stiff passive metal layer of aluminum oxide. Following the removal of the hard oxide liner, chloride ions permeate the FGC via circumferential micro-cracks, resulting in the creation of aluminum chloride by removing hydrogen bubbles. This starts the pitting corrosion process.

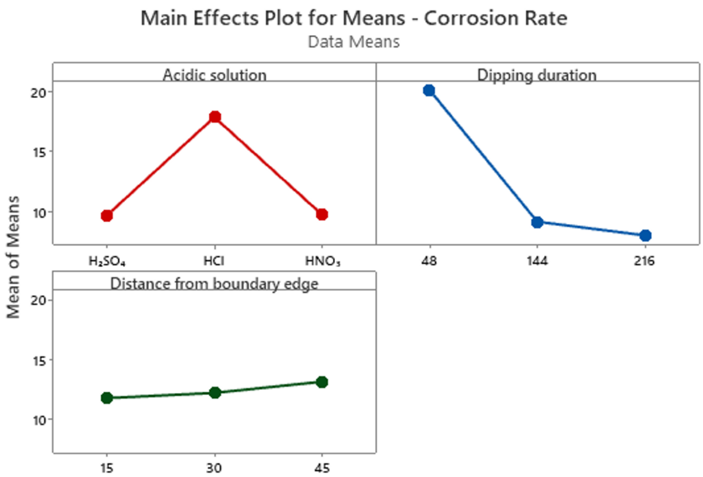

Fig. 5. Influence of corrosion variables on the CR.

The FGC's CR decreased as the falling duration increased. The CR peaks after 48 hours and then rapidly declines at 144 and 216 hours. The absorption of chloride ions improves FGC corrosion resistance after 48 hours of exposure. Corrosion is consistently reduced over a period of 144-216 hours. Regardless of the reinforcement, composite surfaces will form a stable passive layer of aluminum hydroxide. The passive layer may cause the most corrosion during this period. This protective layer stops more rusting in its tracks. The CR of the FGC rose with increasing distance from the border of the boundary. Corrosion occurs more rapidly on the inside than on the outside because of the higher concentration of aggressive ions and the lower ceramic content and passive layer formation on the inside.

The functionally graded distribution of SiC particles also influences corrosion performance, resulting in separate mechanical zones. Higher hardness sections (high particle concentration regions) have denser SiC reinforcement, which acts as a physical barrier, restricting the Al matrix's exposure to corrosive fluids. In contrast, the inner zones (Low particle concentration region) with reduced SiC concentration and hardness provide more favorable pathways for electrolyte penetration, resulting in an increased susceptibility to corrosion. As a result, the mechanical gradient produced by SiC dispersion directly influences the observed discrepancy in corrosion resistance throughout the specimen.

3.5 Worn surface characterization

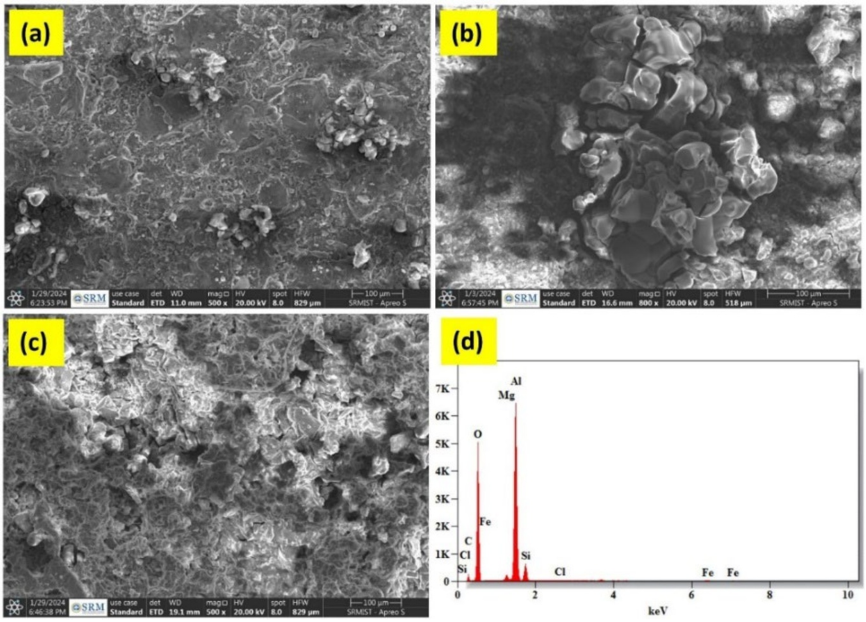

Fig. 6. HRSEM image of the FGC corroded sample surface in (a) H_2SO_4, (b) HCl, (c) HNO_3, and (d) EDS of FGC sample immersed in HCl acidic solution.

Figure 6(a-c) shows the HRSEM image of the FGC corroded sample exterior surface after the immersion in different acidic solution namely H_2SO_4, HCl, and HNO_3, Figure 6(a) shows the HRSEM image of the sample dipped in H_2SO_4 acidic solution and it revealed minimal surface attack due to limited corrosive interaction. Figure 6(b) shows the HRSEM image of the sample dipped in HCl acidic solution and it revealed the severe localized corrosion with preferential aluminum matrix attack around SiC particles due to micro-galvanic effects in an acidic medium. Figure 6(c) shows the HRSEM image of the sample dipped in HNO_3 acidic solution and it revealed the minor attack of the exterior surface owing to its less surface damages. Figure 6(d) shows the EDS of FGC sample immersed in HCl acidic solution. It confirmed the existence of chloride ions through its presence of Cl element in the EDS.

4 Conclusions

Al6061/10 wt.% SiC FGC was efficaciously invented using stir casting continued by vertical centrifugal casting, producing a clear gradient in ceramic particle dissemination from the outer to the inner regions.

Optical microscopy confirmed distinct zones namely high, intermediate, and low particle concentration regions, resulting from centrifugal force and solidification rate differences.

Vickers microhardness was highest near the outer region due to increased SiC particle concentration, demonstrating improved reinforcement dispersion and interfacial bonding.

CR was significantly influenced by acidic solution, dipping duration, and distance from the boundary edge. HCl caused the most severe corrosion, whereas HNO_3 showed the least attack due to passive layer formation.

The CR decreased as the dipping time increased, but it grew in the interior sections, indicating weaker passive layer protection and lower ceramic content far from the boundary edge.

References

1. Bassiouny Saleh, Jinghua Jiang, Reham Fathi, Tareq Al-hababi, Qiong Xu, Lisha Wang, Dan Song, Aibin Ma, 30 Years of functionally graded materials: An overview of manufacturing methods, Applications and Future Challenges. Composites Part B: Engineering. **201**, 108376 (2020). https://doi.org/10.1016/j.compositesb.2020.108376
2. S. Prathap Singh, D. Ananthapadmanaban, N. Venkateshwaran, M. A. Sai Balaji, Effect of Ageing Temperature on the Hardness, Microstructural and Dry Sliding Wear Performance of the Functionally Graded A356 Alloy. Inter Metalcast **19**, 955–976 (2025). https://doi.org/10.1007/s40962-024-01370-0
3. Osama Irfan, Abdualaziz Alaboodi, On the Compression Properties and Erosion-Corrosion Behaviour of Al 6061/15%Sicp Composite. Politeknik Dergisi. **23(2)**, 415-425 (2020). https://doi.org/10.2339/politeknik.535022
4. Bharat Kumar Talluri, R. Narasimha Rao, Mutlu Özcan, P. Syam Prasad, Evaluating mechanical and tribological performance of B4C reinforced aluminum composites with predictive machine learning models. Results in Engineering. **27**, 106503 (2025). https://doi.org/10.1016/j.rineng.2025.106503
5. Şener Karabulut, Halil Karakoç, Musa Bilgin, Hakan Canpolat, Grzegorz M. Krolczyk, Murat Sarıkaya, A comparative study on mechanical and ballistic performance of functionally graded Al6061 composites reinforced with B_4C, SiC, and Al_2O_3. J. Mater. Res. Technol. **23**, 5050-5065 (2023). https://doi.org/10.1016/j.jmrt.2023.02.116
6. Sadanand Sarapure, B. P. Shivakumar, M. B. Hanamantraygouda, Investigation of Corrosion Behavior of SiC-Reinforced Al 6061/SiC Metal Matrix Composites Using Taguchi Technique. J Bio Tribo Corros, 31 (2020). https://doi.org/10.1007/s40735-020-0328-3
7. K. N. Uday, K. Senthilraj, Rajamurugan Govindasamy, Prabu Krishnasamy, Study of NaCl Corrosion Behavior on SiC-Reinforced in Al 6061 and Al 5052 Metal Matrix Composites Using Taguchi's Technique, SAE Technical Paper (2022). https://doi.org/10.4271/2022-28-0531.
8. Rupesh Kumar Verma, Manoj Kumar Chopkar, Dry Sliding Wear Investigation of Centrifugally Casted AA6061–B_4C Functionally Graded Metal Matrix Composite Material by Response Surface Methodology (RSM). Arab J Sci Eng **48**, 4095–4107 (2023). https://doi.org/10.1007/s13369-022-07461-6
9. S. Prathap Singh, D. Ananthapadmanaban, Effect of Silicon Nitride Particles on the Sliding Wear Characteristics of Functionally Graded Aluminium Composite. J. of Materi Eng and Perform **33**, 2875–2896 (2024). https://doi.org/10.1007/s11665-023-09011-z